

## **INFLUENCE OF RESERVOIR AND FOUNDATION ON THE NONLINEAR DYNAMIC RESPONSE OF CONCRETE GRAVITY DAMS**

Rajib Sarkar\*, D.K. Paul\* and L. Stempniewski\*\*

\*Department of Earthquake Engineering  
IIT Roorkee, Roorkee-247 667

\*\*Institute for Solid Constructions and Building Materials  
University of Karlsruhe, Germany

### **ABSTRACT**

The dynamic analysis of a concrete gravity dam is a reasonably complex problem. The response of a dam subjected to dynamic loading is a combined effect of the interaction among dam, reservoir and foundation systems. The profile of the Koyna dam has been adopted for the study of this investigation. Nonlinear concrete properties have been taken into account through concrete damaged plasticity model to simulate the damage induced in the dam body under a real-time earthquake motion. The study indicates that tensile damage of the dam structure occurred during the earthquake motion. Parametric studies, while varying the height of the reservoir and the foundation modulus values, have been conducted to show the influence of reservoir and foundation material on the dynamic response of concrete gravity dams.

**KEYWORDS:** Dam, Reservoir, Foundation, Interaction, Damage

### **INTRODUCTION**

The Koyna hydro-electric project is situated in Maharashtra, India, approximately 200 km from Mumbai. This project primarily envisages generation of power, with some irrigation on the banks of river Krishna. The principal feature of the project is the Koyna dam which is a gravity structure. The highest monolith of this structure is 103 m high and 70 m wide. A severe earthquake (of Richter magnitude 6.5), which occurred on December 11, 1967 with its epicentre very close to the dam, caused damage to the dam. During this earthquake, the higher monoliths of the non-overflow section suffered severe distress. Structural cracking of the concrete on the upstream as well as on the downstream face occurred in the region of 66.5 m elevation where the downstream slope undergoes a change. With the occurrence of severe earthquakes leading to distress in many dams, it becomes necessary to review the behavior of dams in a seismic environment.

Linear analyses (Chopra and Chakrabarti, 1972) reveal that large tensile stresses in excess of the strength of the concrete would develop in the dam during strong earthquakes. Following this, many nonlinear analyses have been carried out to predict the occurrence and propagation of cracks.

Using the maximum tensile strength criteria Skrikerud and Bachmann (1986) simulated the crack propagation of the Koyna dam under strong earthquakes by incorporating the discrete crack approach in a finite element program.

Droz (1987) investigated the seismic fracture response of a concrete gravity dam using the linear elastic fracture mechanics propagation criterion. The crack profiles were spatially represented using finite element formulations based on discontinuous shape functions. This approach is conceptually equivalent to that of discrete crack models. The analysis predicted localized cracks propagating deep inside the dam.

El-Aidi and Hall (1989a, 1989b) studied possible seismic cracking of Pine Flat dam using the smeared crack approach. The crack profile determined from an automated analysis was reported to be unrealistic. The choice of analyst was therefore incorporated in the solution procedure to guide the smeared crack profile in the desired direction.

Ayari and Saouma (1990) applied a linear elastic fracture mechanics criterion with the discrete crack model for seismic analysis of the Koyna dam. Cracks were predicted on upstream and downstream faces at the elevation of sharp change in the downstream slope.

The seismic response of the Pine Flat dam was also investigated by Feltrin et al. (1992). Crack-interlock elements were introduced along the inter-element discrete cracks to model the aggregate interlock mechanism that caused significant branching of the primary crack profile.

Bhattacharjee and Leger (1993) applied a nonlinear smeared fracture model for predicting the seismic cracking and energy response of concrete gravity dams. A plane-stress finite element idealization had been adopted for the seismic fracture analysis of concrete gravity dams. This smeared crack analysis model is based on the nonlinear fracture behavior of concrete considering the strain-softening behavior in the fracture zone.

Ghrib and Tinawi (1995) contributed to this area of research by introducing damage mechanics into such analyses. A local approach for the nonlinear response of concrete gravity dams was also presented.

All these studies have demonstrated the formation of cracks on both faces during the 1967 Koyna earthquake. However the studies by Bhattacharjee and Leger (1993) and Ghrib and Tinawi (1995) showed that damage would occur at the heel of the dam also. Further, all of these studies either considered no reservoir condition or considered added lump mass model for the incompressible reservoir water. The foundation was considered to be rigid.

The model used in this study considers compressible reservoir water and linear elastic homogeneous foundation material. Throughout this study, analyses are performed by the software ABAQUS (Version 6.5). The tensile damage in concrete under dynamic condition is simulated by the plasticity model proposed by Lubliner et al. (1989) and Lee and Fenves (1998) and incorporated in ABAQUS.

## CONCRETE DAMAGED PLASTICITY MODEL

The concrete damaged plasticity model, which has been used to simulate the nonlinear properties of the concrete, is described briefly in this section. This model is primarily intended to provide a general capability for the analysis of concrete structures under cyclic and/or dynamic loading. Under low confining pressures concrete behaves in a brittle manner; the main failure mechanisms being (a) cracking in tension, and (b) crushing in compression. The brittle behavior of concrete disappears when the confining pressure is sufficiently large to prevent crack propagation. In these circumstances the failure is driven by the consolidation and collapse of the concrete microporous microstructure, leading to a macroscopic response that resembles that of a ductile material with work hardening.

The constitutive theory of the model used aims to capture the effects of irreversible damage associated with the failure mechanisms that occur in concrete under fairly low confining pressures. These effects manifest themselves in the following macroscopic properties:

- different yield strengths in tension and compression, with the initial yield stress in compression being higher than the initial yield stress in tension by a factor of 10 or more;
- softening behavior in tension as opposed to the initial hardening followed by softening in compression;
- different degradations of the elastic stiffness in tension and compression;
- stiffness recovery effects during cyclic loading; and
- rate sensitivity, especially an increase in the peak strength with strain rate.

This model cannot take into account the anisotropy of the material and the shear strength of the cracked section. These are the main limitations of the model. An overview of this model is given below.

### 1. Damage and Stiffness Degradation

Damaged states in tension and compression are characterized independently by two hardening variables,  $\tilde{\epsilon}_t^{pl}$  and  $\tilde{\epsilon}_c^{pl}$ , which are referred to as equivalent plastic strains in tension and compression, respectively. The evolution equations of the hardening variables,  $\tilde{\epsilon}_t^{pl}$  and  $\tilde{\epsilon}_c^{pl}$ , are conveniently formulated by considering uniaxial loading conditions first and then extended to multi-axial conditions.

### 2. Uniaxial Conditions

It is assumed that the uniaxial stress-strain curves can be converted into stress versus plastic strain curves of the form,

$$\begin{aligned} \sigma_t &= \sigma_t(\tilde{\varepsilon}_t^{pl}, \dot{\tilde{\varepsilon}}_t^{pl}, \theta, f_i) \\ \sigma_c &= \sigma_c(\tilde{\varepsilon}_c^{pl}, \dot{\tilde{\varepsilon}}_c^{pl}, \theta, f_i) \end{aligned} \tag{1}$$

where the subscripts  $t$  and  $c$  refer to tension and compression, respectively;  $\tilde{\varepsilon}_t^{pl}$  and  $\tilde{\varepsilon}_c^{pl}$  are the equivalent plastic strain rates;  $\tilde{\varepsilon}_t^{pl} = \int_0^t \dot{\tilde{\varepsilon}}_t^{pl} dt$  and  $\tilde{\varepsilon}_c^{pl} = \int_0^t \dot{\tilde{\varepsilon}}_c^{pl} dt$  are the equivalent plastic strains;  $\theta$  is the temperature; and  $f_i$  ( $i=1, 2, \dots$ ) are other predefined field variables.

If  $\dot{\varepsilon}_{11}^{pl}$  is the strain rate, the effective plastic strain rates under uniaxial loading conditions are given as

$$\dot{\tilde{\varepsilon}}_t^{pl} = \dot{\varepsilon}_{11}^{pl} \text{ (in uniaxial tension)}$$

and (2)

$$\dot{\tilde{\varepsilon}}_c^{pl} = -\dot{\varepsilon}_{11}^{pl} \text{ (in uniaxial compression)}$$

As shown in Figure 1, when the concrete specimen is unloaded from any point on the strain-softening branch of the stress-strain curve, the unloading response is observed to be weakened: the elastic stiffness of the material appears to be damaged (or degraded). The degradation of the elastic stiffness is significantly different between the tension and compression cases. The degraded response of concrete is characterised by two independent uniaxial damage variables,  $d_t$  and  $d_c$ , which are assumed to be functions of the plastic strains, temperature, and field variables:

$$\begin{aligned} d_t &= d_t(\tilde{\varepsilon}_t^{pl}, \theta, f_i), \quad 0 \leq d_t \leq 1 \\ d_c &= d_c(\tilde{\varepsilon}_c^{pl}, \theta, f_i), \quad 0 \leq d_c \leq 1 \end{aligned} \tag{3}$$

The uniaxial degradation variables are increasing functions of the equivalent plastic strains. They can take values ranging from zero, for the undamaged material, to one, for the fully damaged material.

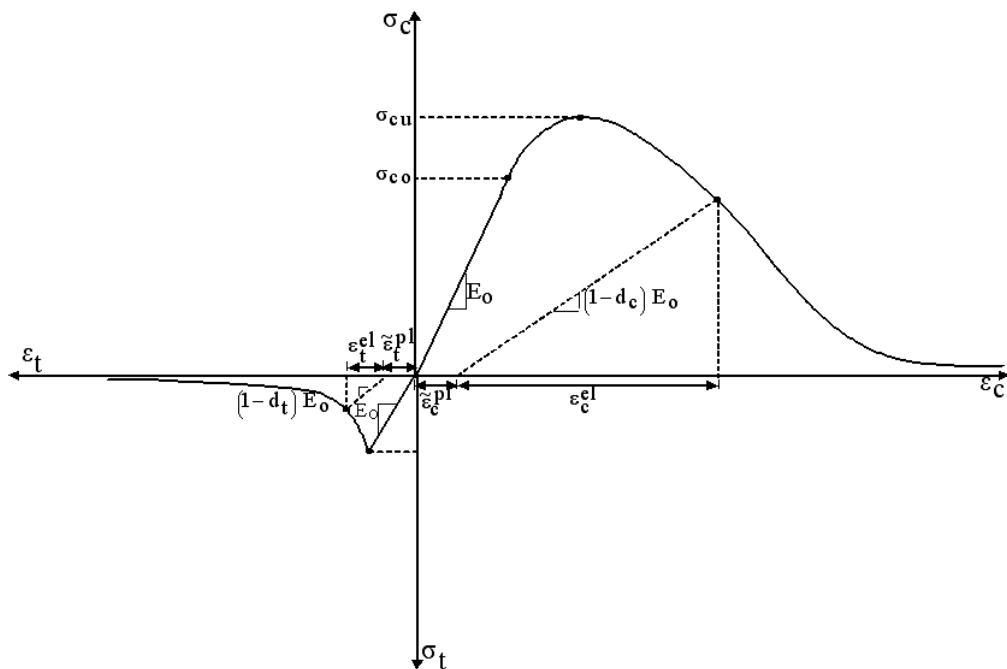


Fig. 1 Response of concrete to uniaxial loading in compression and tension

If  $E_0$  is the initial (undamaged) elastic stiffness of the material, the stress-strain relations under uniaxial tension and compression loading are, respectively,

$$\begin{aligned}\sigma_t &= (1 - d_t) E_0 (\varepsilon_t - \tilde{\varepsilon}_t^{pl}) \\ \sigma_c &= (1 - d_c) E_0 (\varepsilon_c - \tilde{\varepsilon}_c^{pl})\end{aligned}\tag{4}$$

Under uniaxial tensile loading, damage propagates in a direction transverse to the stress direction. The nucleation and propagation of damage, therefore, causes a reduction of the available load-carrying area, which in turn leads to an increase in the effective stress. This effect is less pronounced under compressive loading since damage runs parallel to the loading direction; however, after a significant amount of crushing, the effective load-carrying area is significantly reduced. The effective uniaxial stresses,  $\bar{\sigma}_t$  and  $\bar{\sigma}_c$ , are

$$\begin{aligned}\bar{\sigma}_t &= \frac{\sigma_t}{1 - d_t} = E_0 (\varepsilon_t - \tilde{\varepsilon}_t^{pl}) \\ \bar{\sigma}_c &= \frac{\sigma_c}{1 - d_c} = E_0 (\varepsilon_c - \tilde{\varepsilon}_c^{pl})\end{aligned}\tag{5}$$

To avoid unreasonable mesh-sensitive results due to the lack of reinforcement in the structure, the tensile post-failure behaviour is given in terms of a fracture energy cracking criterion by specifying a stress-displacement curve instead of a stress-strain curve, as shown in Figure 3. The values of  $\bar{\sigma}_t$  and  $\bar{\sigma}_c$  are determined following the experimental and numerical results presented by Lee and Fenves (1998).

It is well known that the materials such as concrete can exhibit a significant volume change when subjected to severe inelastic states. This change in volume, caused by the plastic distortion, can be reproduced well by using an adequate plastic potential function  $G$  in the definition of the plastic-flow rule (Lubliner et al., 1989). For  $G$ , the classical Mohr-Coulomb yield function with the angle of dilatancy  $\psi$  is

$$G(\sigma, \psi) = \frac{I_1}{3} \sin \psi + \sqrt{J_2} \left( \cos \theta - \frac{\sin \theta \sin \psi}{\sqrt{3}} \right)\tag{6}$$

where  $J_2$  is the second invariant of stress deviator,  $I_1$  is the first invariant of stress, and the third invariant enters through the polar angle  $\theta$  in the deviatoric plane.

Under multiaxial cyclic loading conditions the degradation mechanisms are quite complex, involving the opening and closing of previously formed micro-cracks, as well as their interaction. However, the fundamentals of the model are the same as stated for the uniaxial conditions. Experimentally, it is observed that there is some recovery of the elastic stiffness as the load changes sign during a uniaxial cyclic test. The stiffness recovery effect, also known as the “unilateral effect”, is an important aspect of the concrete behavior under cyclic loading. This effect is usually more pronounced as the load changes from tension to compression, causing tensile cracks to close, which results in the recovery of the compressive stiffness. This behavior is also implemented in the model considered. Then it is extended for the multi-axial conditions (Lee and Fenves, 1998).

## SYSTEM ANALYSED

The geometry of a typical non-overflow monolith of the Koyna dam-reservoir-foundation is illustrated in Figure 2. This monolith is 103 m high and 70 m wide at its base (Chopra and Chakrabarti, 1972). The upstream wall of the monolith is assumed to be straight and vertical which is slightly different from the real configuration. The depth of the reservoir at the time of the earthquake was 91.75 m. Following the work of other investigators (e.g., Hall, 1986), the non-overflow monolith of the dam is assumed to be in the plane-stress condition. First-order and plane-stress elements have been used to model the dam body. The dam is assumed to rest on a 350×140 m foundation. The bottom of the foundation is assumed to be fixed and the foundation is considered to be in the plane-strain condition (Hall, 1986). First-order and plane-strain elements have been used for modelling the foundation. Infinite element boundary conditions have been used at the ends of the foundation block to simulate the unbounded nature of the foundation. The use of infinite elements for the simulation of unbounded nature of the medium has been explained by Zienkiewicz et al. (1983) for static as well as dynamic conditions. For the static

response of infinite elements, the solution in the far field is assumed to be linear. The dynamic response of infinite elements is based on the consideration of plane body waves traveling orthogonally to the boundary. The response adjacent to the boundary is assumed to be of small enough amplitude so that the medium responds in a linear elastic fashion. First-order, plane-strain infinite elements have been used on each side. The reservoir is assumed to be 140 m in length, and first-order acoustic elements (with velocity-pressure formulation same as the Lagrange multiplier formulation wherein the constraint is introduced by means of the Lagrange multiplier) have been used for the reservoir. Linear acoustic infinite elements have been used as the boundary of the upstream side of the reservoir.

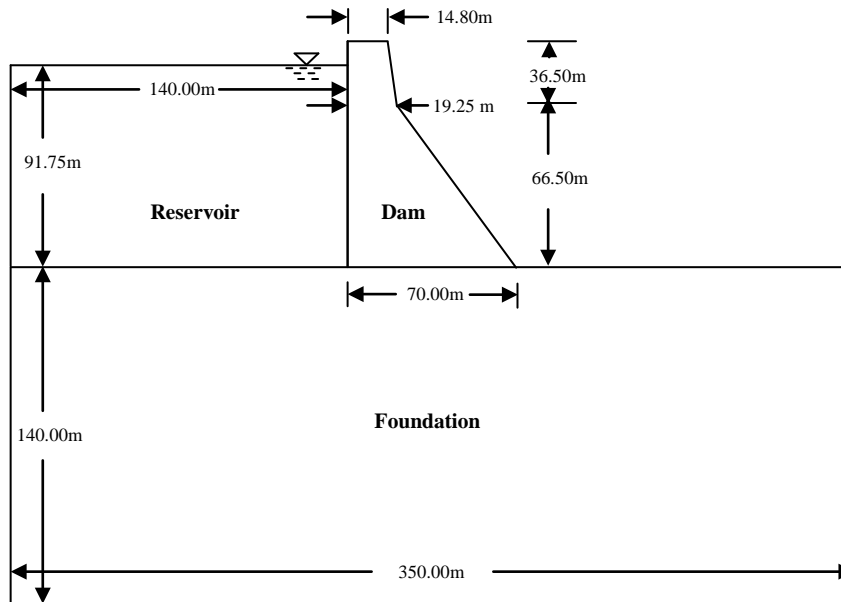


Fig. 2 Dam-reservoir-foundation system

**1. Reservoir Water Modelling**

Hall (1986) stated with reason that a lumped, added mass approach of Westergaard using incompressible water is less accurate than a model using finite element model with compressible water. In this study, the reservoir water has been taken as a compressible, inviscid fluid.

The free-surface condition assumes that the surface pressure is always equal to the atmospheric pressure, thus neglecting the free-surface water waves.

Chopra (1968), through a frequency-domain study, has demonstrated that water compressibility should not be important in the earthquake response of concrete gravity dams if the ratio  $\omega_w/\omega_d$  exceeds 2, where  $\omega_w$  and  $\omega_d$  are the fundamental resonance frequencies of the water and the dam without water, respectively. Here, for 91.75 m reservoir height,  $\omega_w = 4.087$  Hz, and for dam,  $\omega_d = 3.002$  Hz, and thus,  $\omega_w/\omega_d$  equals 1.36.

**2. Boundary Impedance**

Boundary impedance specifies relationship between the pressure of a fluid medium and the normal motion at the reservoir-foundation interface boundary. The impedance boundary condition at any point along the fluid-medium surface is governed by

$$\dot{u}_{out} = \frac{p}{c_1} \tag{7}$$

where  $\dot{u}_{out}$  is the particle velocity in the outward normal direction of the fluid-medium surface,  $p$  the fluid pressure, and  $1/c_1 = 1/\rho_f c_f$  the proportionality coefficient between the pressure and the velocity normal to the surface. Further,  $\rho_f$  is the density of the foundation, and  $c_f$  is the velocity of compression

waves in the foundation material. This model can be conceptualized as dashpots placed in series between the fluid medium and the foundation. The dashpot parameter is  $c_1$ , defined per unit area of the interface surface. Coupling with the motion of the dam structure, as described by the displacements, occurs on the boundary between the reservoir and the dam.

**PARAMETERS**

Parameters of the Koyna dam considered are (Bhattacharjee and Leger, 1993; Ghrib and Tinawi, 1995; Skrikerud and Bachmann, 1986): elastic modulus  $E_d = 31027$  MPa, mass density  $\rho_c = 2643$  kg/m<sup>3</sup>, Poisson’s ratio  $\nu_c = 0.2$ , dilatation angle  $\psi_c = 36.31^\circ$ , compressive initial yield stress  $\sigma_{co} = 13.0$  MPa, compressive ultimate stress  $\sigma_{cu} = 24.1$  MPa, tensile failure stress  $\sigma_{to} = 2.9$  MPa. The tensile post-failure behavior has been determined following Lee and Fenves (1998), and is given by specifying a stress-displacement curve, as shown in Figure 3(a). Tensile damage is specified in tabular form as a function of cracking displacement and is shown in Figure 3(b). The stiffness degradation damage caused by the compressive failure (crushing) of the concrete is assumed to be zero.

The first four fundamental natural frequencies of the finite element model of only the dam structure, i.e., 3.002, 7.953, 10.848, and 15.640 Hz, are consistent with those reported in the literature (Bhattacharjee and Leger, 1993; Chopra and Chakrabarti, 1973; Ghrib and Tinawi, 1995).

Parameters of the reservoir water are: bulk modulus  $K_w = 2250$  MPa, and mass density  $\rho_w = 1000$  kg/m<sup>3</sup>. The foundation material is assumed to be linearly elastic. The foundation parameters are: elastic modulus  $E_f = 62054$  MPa, mass density  $\rho_f = 3300$  kg/m<sup>3</sup>, and Poisson’s ratio  $\nu_f = 0.33$ .

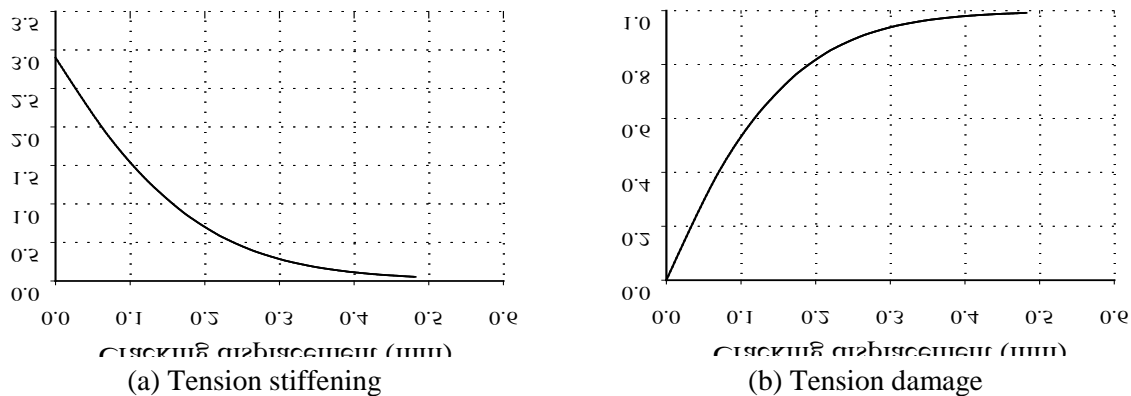


Fig. 3 Tensile material properties of concrete

Stiffness-proportional damping appeals to the intuition because it can be interpreted to model the energy dissipation arising from the deformations. In contrast, a mass-proportional damping is difficult to justify physically because the air damping, it can be interpreted to model, is negligibly small for most structures (Chopra, 2001). In this study material damping is taken as proportional to stiffness, and the factor of stiffness-proportional damping is given by

$$a_1 = \frac{2\xi_j}{\omega_j} \tag{8}$$

Here  $\xi_j$  and  $\omega_j$ , respectively, are the damping ratio and natural frequency for the  $j$ th mode.

It is generally accepted that dams have damping ratios of about 2–5%. The material damping properties are tuned to provide a 5% of critical damping for the first mode of vibration, i.e.,  $\xi_1 = 0.05$ , and the factor of stiffness-proportional damping for the first natural mode is 0.053 s.

## GROUND MOTIONS

For this study, the horizontal and vertical acceleration records of 1967 Koyna earthquake have been used. These records are shown in Figure 4.

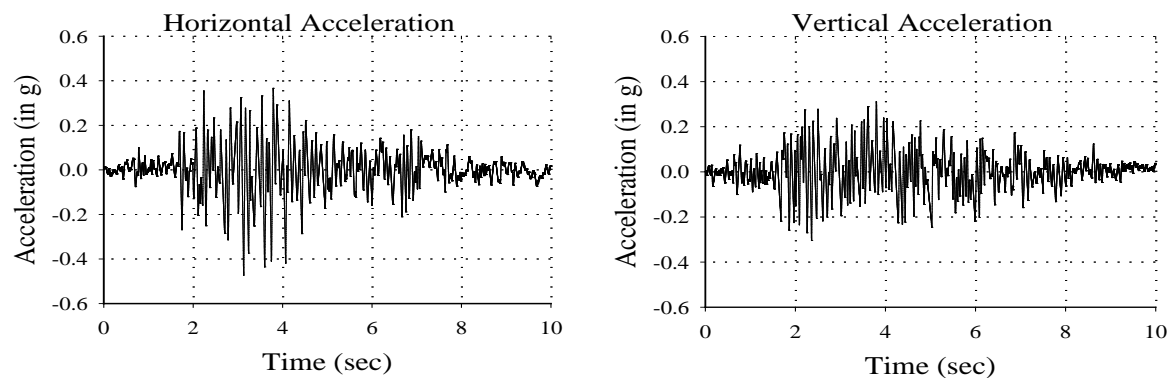


Fig. 4 1967 Koyna earthquake accelerations

## LOADING AND SOLUTION CONTROL

Prior to the dynamic simulation, the model is subjected to gravity loading and hydrostatic pressure along the dam-reservoir interface. In the analyses these loads are specified in two consecutive static steps. For the dynamic analysis, in the third step the horizontal and vertical components of the deconvolved ground accelerations are applied to all nodes at the base of the foundation. Uplift pressures have not been included.

For determining the time increment of the analysis, a comparison has been done taking time increments of 0.01 and 0.001 s, respectively. Effect of mesh size has also been examined and correspondingly mesh has been refined. This comparison shows that the responses are converging. A time increment of 0.01 s has been used for the study. The Hilbert-Hughes-Taylor operator, which is implicit in nature, was used as the time integration scheme.

## RESPONSE QUANTITIES

To show the influence of foundation interaction as well as reservoir interaction on the response of the dam three different systems have been considered. These systems are given below:

- System 1: Only the dam structure fixed at its base.
- System 2: The dam with the foundation block fixed at the bottom of its foundation.
- System 3: The entire dam-reservoir-foundation system.

These three systems have been analysed in time domain using the Koyna earthquake acceleration records as the input motion.

The following response quantities for these systems have been compared:

- accelerations at the crest of the dam;
- displacements at the crest of the dam; and
- stresses at the heel of the dam.

The quantitative comparisons among the peak values of different response quantities for different systems show (see Table 1) that the stresses and displacements, which are two basic responses, get changed significantly with the consideration of the foundation and the reservoir.

Figure 5 shows the responses of the dam-reservoir-foundation system. It may be seen that the displacement response at the crest and stress response at the heel begin from some initial values. This is due to the initial values due to the static loading before the dynamic loading. The plots of stresses at the heel also show that after some time interval, stresses reduce suddenly. It is due to the tensile damage at the heel for concrete nonlinearity. It may be concluded from the plots that concrete loses its strength at those damaged locations to take the tensile loads coming due to the dynamic loading of the system.

Table 1: Peak Values of Responses for Different Systems

Systems	Crest Acceleration (m/s <sup>2</sup> )		Crest Displacement (cm)		Heel Stress (MPa)		
	Horz.	Vert.	Horz.	Vert.	$S_{11}$	$S_{12}$	$S_{22}$
System 1	15.89	10.93	3.38	1.25	0.71	0.85	3.15
System 2	16.10	11.25	4.48	1.68	0.92	1.13	5.29
System 3	15.51	10.18	6.13	1.70	1.10	1.12	8.37

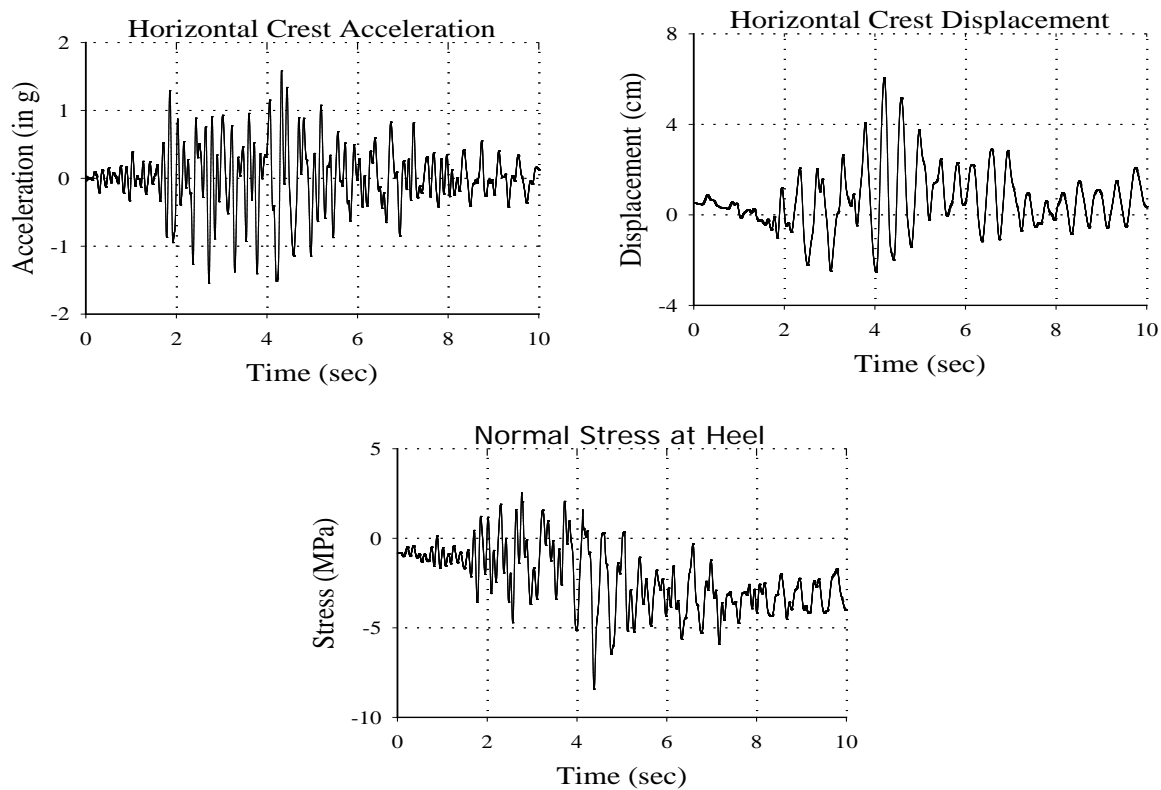


Fig. 5 Response quantities for the dam-reservoir-foundation system

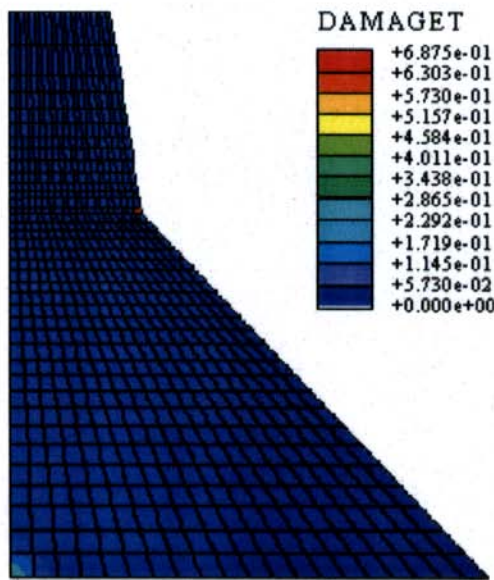
## DAMAGE IN DAM

The constitutive model used here simulates the tensile damage patterns based on the stress-strain curve of the concrete shown in Figure 1. The parameter DAMAGET shown in Figures 6–8 indicates the degradation variable  $d_t$ , described in Equation (3). It may be mentioned that if DAMAGET = 1.0, the effective stress  $\bar{\sigma}_t$  tends to infinity as per Equation (5), which the described material model cannot take into account. Thus it may be stated that the exponential nature of the tensile stress-strain curve (as in Figure 1) is not realistic in simulating the concrete crack openings. The described material model however simulates the tensile damage patterns in the Koyna concrete dam reasonably well.

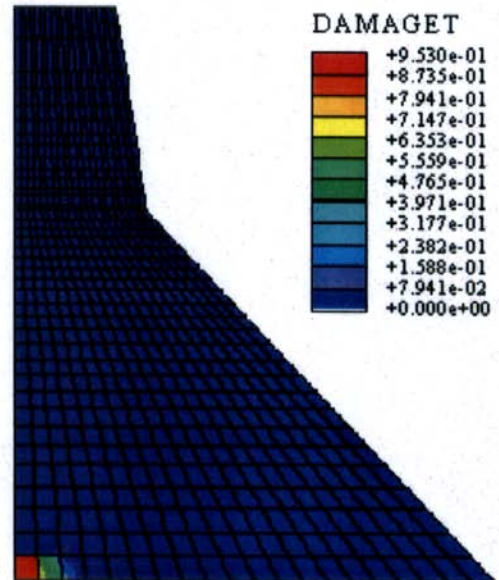
The initiation and the propagation of the regions of tensile damage for Systems 1, 2 and 3 are shown in Figures 6–8. The tensile damage in the dam structure only (i.e., System 1) and in the dam with foundation (i.e., System 2) is initiated at the point where the slope changes in the downstream direction, and propagates towards the upstream direction. The region near the heel of the dam also gets damaged for both systems. These patterns of damage match with the results available in the literature (Bhattacharjee and Leger, 1993; Feltrin et al., 1992).



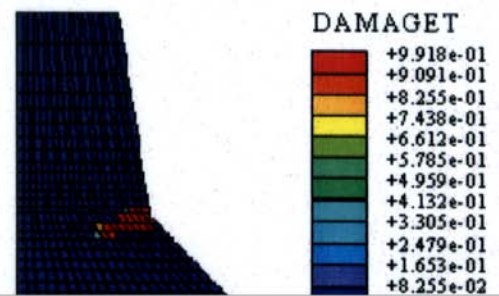
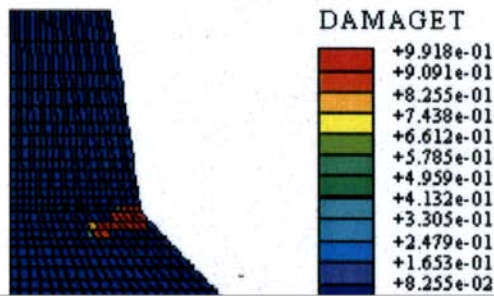
However, when the reservoir is taken into account, the dam exhibits a different damage pattern. This is because of the interaction of compressible water with the dam structure, which results in hydrodynamic pressures. The impulsive pressures, which are experienced by a dam in the event of an earthquake, are the main cause of these pressures. In this case, the tensile damage starts at the point of change of slope in the downstream direction but it mainly occurs at nearly the same level in the upstream direction. This pattern of damage is somewhat different from that reported earlier in the literature. This is due to the fact that most of the earlier efforts either used an added lump mass model for the incompressible reservoir water or assumed the rigid foundation condition.



(a) Time step= 3.9sec



(b) Time step= 4.2sec



(c) Time step= 4.4sec

(d) Time step= 10.0sec

Fig. 6 Formation and propagation of tensile damage for System 1

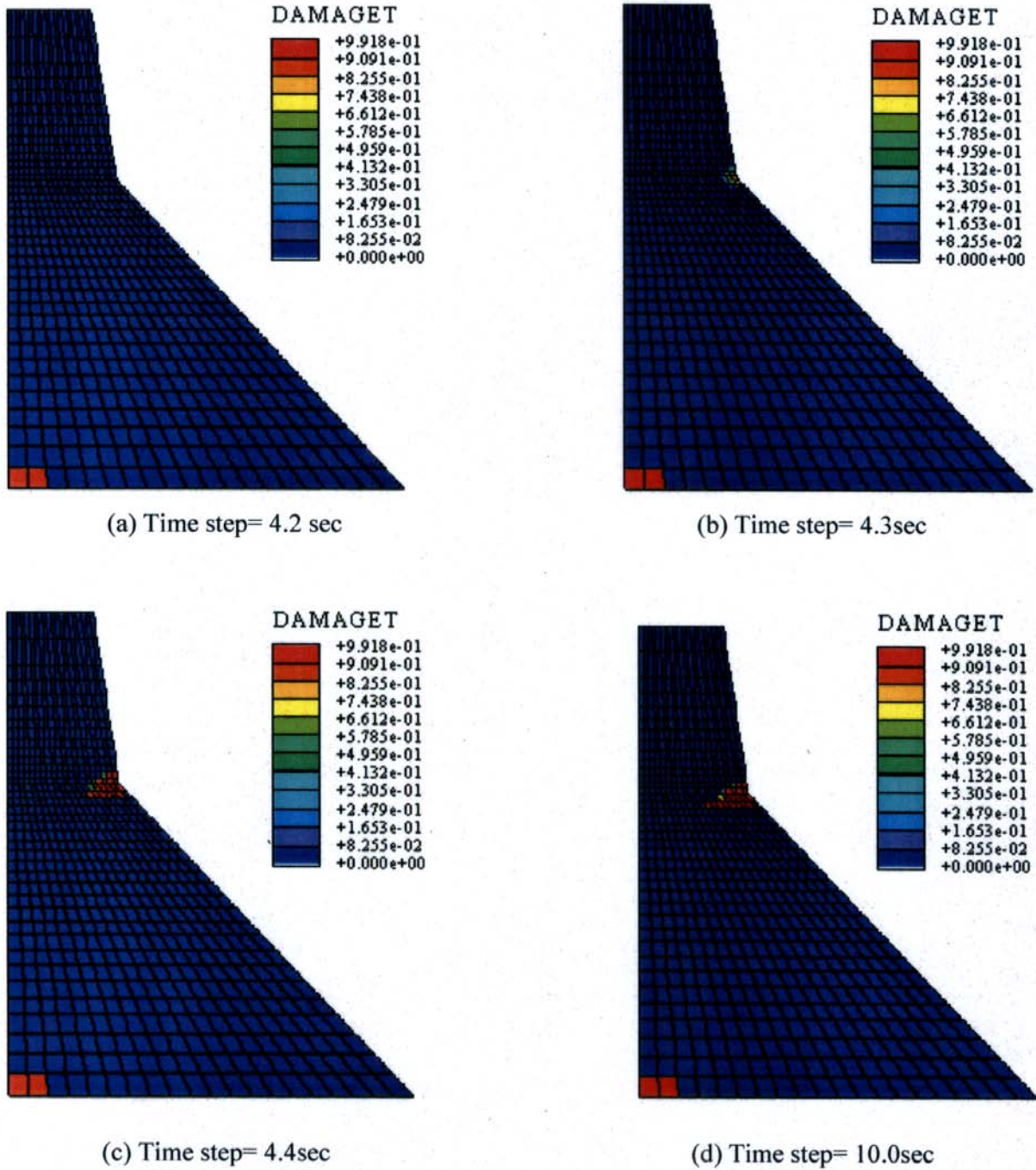


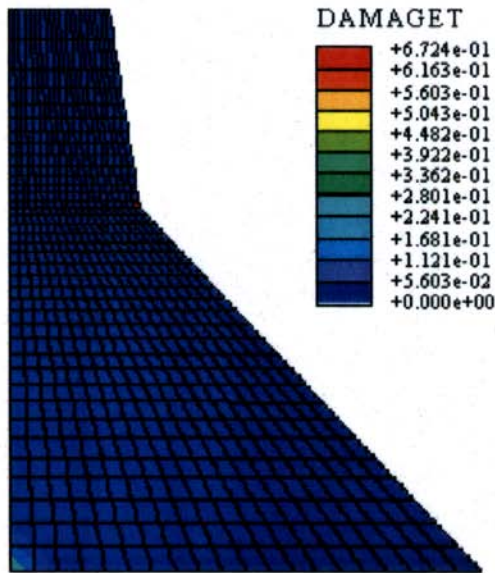
Fig. 7 Formation and propagation of tensile damage for System 2

**PARAMETRIC STUDIES**

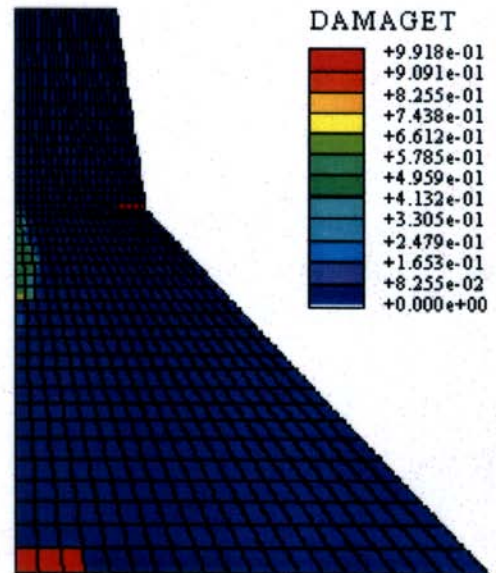
The most important parameters influencing the response of dam on rigid foundation are  $E_d$ , the Young’s modulus of elasticity for mass concrete in the dam structure, and  $H/H_d$ , the ratio of water depth to the dam height. When dam-foundation interaction is considered, an additional parameter becomes important:  $E_f/E_d$ , the ratio of Young’s moduli for the foundation and dam materials. For a fixed value of  $E_f/E_d$ , the value of  $E_d$  influences the response of the structure to a minor extent for horizontal ground motions and significantly for vertical ground motions. However, the Young’s modulus of concrete has been kept constant in this study, and for parametric studies the complete dam-reservoir-foundation system with nonlinearity introduced in the concrete has been considered.

### 1. Variation of Foundation Modulus

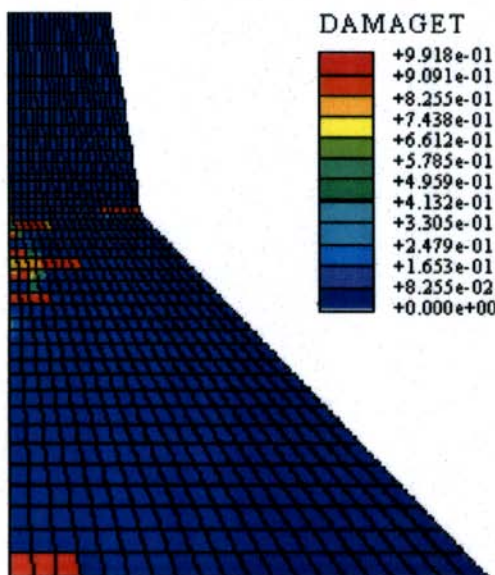
The responses of the dam have been found out for different values of foundation modulus. Results are presented for five values of  $E_f/E_d$  : 4, 2, 1,  $\frac{1}{2}$  and  $\frac{1}{4}$ . The first value represents almost rigid foundation. In the last two cases, the elastic modulus for the foundation material is a fraction of the modulus for dam concrete, which may be appropriate in many situations because of the joints in the foundation rock. Analyses have been done in time domain for the different values of foundation modulus. The results show that the crest displacements go on increasing with decrease in foundation modulus. This observation is similar to the analyses in frequency domain (Chopra and Gupta, 1982; Hall, 1986). A comparison of the peak values of different response quantities of the dam structure is provided in Table 2.



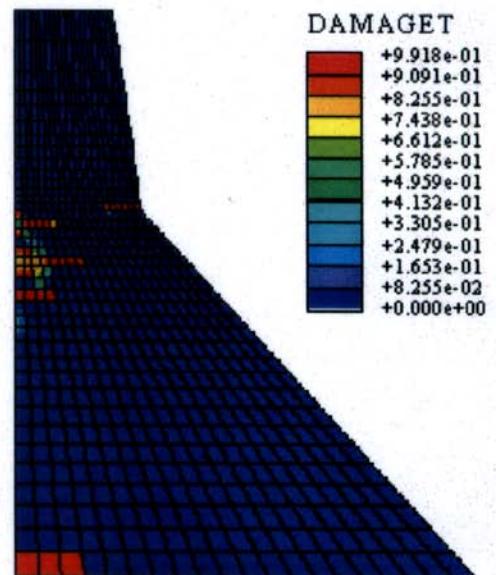
(a) Time step= 2.8sec



(b) Time step= 4.2sec



(c) Time step= 4.3sec



(d) Time step= 10.0sec

Fig. 8 Formation and propagation of tensile damage for System 3

**Table 2: Peak Values of Responses for Different Foundation Moduli**

$E_f/E_d$	Crest Acceleration (m/s <sup>2</sup> )		Crest Displacement (cm)		Heel Stress (MPa)		
	Horz.	Vert.	Horz.	Vert.	$S_{11}$	$S_{12}$	$S_{22}$
4	16.70	14.10	5.73	1.40	0.84	1.23	7.89
2	15.50	10.20	6.13	1.70	1.10	1.12	8.37
1	17.60	7.57	7.09	2.82	1.59	1.29	7.70
1/2	14.70	7.26	7.32	4.16	1.73	1.18	7.60
1/4	11.40	6.37	8.96	6.61	1.11	1.24	6.44

## 2. Variation of Reservoir Depth

By changing the reservoir depth, different dam responses have been calculated. Results are presented for three values of  $H_{rp}/H_{rf}$ : 0, 0.7 and 1, where  $H_{rp}$  denotes the partial reservoir depth and  $H_{rf}$  the full reservoir depth. It is seen that the responses increase with the height of the reservoir but for  $H_{rp}/H_{rf}$  less than 0.7, the height of reservoir has hardly any effect on the response of the dam structure. This can be seen in the frequency domain studies (e.g., Chopra and Gupta, 1982) as well as in the time history analysis of this study. A comparison of the peak values of different response quantities of the dam structure is provided in Table 3.

**Table 3: Peak Values of Responses for Different Reservoir Depths**

$H_{rp}/H_{rf}$	Crest Acceleration (m/s <sup>2</sup> )		Crest Displacement (cm)		Heel Stress (MPa)		
	Horz.	Vert.	Horz.	Vert.	$S_{11}$	$S_{12}$	$S_{22}$
0.0	16.10	11.20	4.48	1.68	0.92	1.13	5.29
0.7	15.70	10.30	4.81	1.68	1.03	1.02	6.46
1.0	15.50	10.20	6.13	1.70	1.10	1.12	8.37

## SUMMARY AND CONCLUSIONS

The earthquake response of concrete gravity dam-reservoir-foundation system has been investigated with emphasis on the nonlinear behavior associated with concrete tensile damage. For the sake of simplicity, the dam has been idealised by considering only a separate monolith under the plane-stress condition, and the two-dimensional assumption has been extended to model the compressible infinite reservoir domain. The dam-reservoir system has been treated as an integral system. Along the foundation-reservoir interface, the absorbing boundary condition has been used. Viscous damping in the form of stiffness-proportional damping has been used. Energy dissipation in the reservoir domain and the unbounded foundation medium has been accounted for through infinite elements. No uplift pressure has been introduced in the model. Based on these, the following main conclusions are drawn:

- As expected, the behavior of dam structure under earthquake largely depends on the foundation and the reservoir. With a decrease in the foundation modulus, the displacements increase. If reservoir depth is less than 0.7 times the full-reservoir depth, the reservoir has no significant impact on the dynamic behavior of the dam structure.
- The tensile damage patterns of the systems considering (i) only the dam structure, and (ii) the dam with the foundation, are almost same. But when the reservoir is considered along with the dam and the foundation, the damage pattern obtained is somewhat different. It shows that the crack initiates at the point of slope change in the downstream side of the dam structure and then grows at nearly the

same level. However, this happens in the upstream side of the dam structure and this is due to impulsive pressures of the reservoir water on the dam.

## REFERENCES

1. Ayari, M.L. and Saouma, V.E. (1990). "A Fracture Mechanics Based Seismic Analysis of Concrete Gravity Dams Using Discrete Cracks", *Engineering Fracture Mechanics*, Vol. 35, No. 1-3, pp. 587–598.
2. Bhattacharjee, S.S. and Leger, P. (1993). "Seismic Cracking and Energy Dissipation in Concrete Gravity Dams", *Earthquake Engineering & Structural Dynamics*, Vol. 22, No. 11, pp. 991–1007.
3. Chopra, A.K. (1968). "Earthquake Behavior of Reservoir-Dam Systems", *Journal of the Engineering Mechanics Division, Proceedings of ASCE*, Vol. 94, No. EM6, pp. 1475–1500.
4. Chopra, A.K. (2001). "Dynamics of Structures: Theory and Applications to Earthquake Engineering", Prentice Hall, Upper Saddle River, U.S.A.
5. Chopra, A.K. and Chakrabarti, P. (1972). "The Earthquake Experience at Koyna Dam and Stresses in Concrete Gravity Dams", *Earthquake Engineering & Structural Dynamics*, Vol. 1, No. 2, pp. 151–164.
6. Chopra, A.K. and Chakrabarti, P. (1973). "The Koyna Earthquake and the Damage to Koyna Dam", *Bulletin of the Seismological Society of America*, Vol. 63, No. 2, pp. 381–397.
7. Chopra, A.K. and Gupta, S. (1982). "Hydrodynamic and Foundation Interaction Effects in Frequency Response Functions for Concrete Gravity Dams", *Earthquake Engineering & Structural Dynamics*, Vol. 10, No. 1, pp. 89–106.
8. Droz, P. (1987). "Modele Numerique du Comportement Non-lineaire D'ouvrages Massifs en Beton Non Arme", Thesis No. 682, Département de Génie Civil, Ecole Polytechnique Fédérale de Lausanne, Lausanne, Switzerland (in French).
9. El-Aidi, B. and Hall, J.F. (1989a). "Non-linear Earthquake Response of Concrete Gravity Dams Part 1: Modelling", *Earthquake Engineering & Structural Dynamics*, Vol. 18, No. 6, pp. 837–851.
10. El-Aidi, B. and Hall, J.F. (1989b). "Non-linear Earthquake Response of Concrete Gravity Dams Part 2: Behaviour", *Earthquake Engineering & Structural Dynamics*, Vol. 18, No. 6, pp. 853–865.
11. Feltrin, G., Galli, M. and Bachmann, H. (1992). "Influence of Cracking on the Earthquake Response of Concrete Gravity Dams with Reservoir", *Proceedings of the Tenth World Conference on Earthquake Engineering*, Madrid, Spain, Vol. 8, pp. 4627–4632.
12. Ghrib, F. and Tinawi, R. (1995). "An Application of Damage Mechanics for Seismic Analysis of Concrete Gravity Dams", *Earthquake Engineering & Structural Dynamics*, Vol. 24, No. 2, pp. 157–173.
13. Hall, J.F. (1986). "Study of the Earthquake Response of Pine Flat Dam", *Earthquake Engineering & Structural Dynamics*, Vol. 14, No. 2, pp. 281–295.
14. Lee, J. and Fenves, G.L. (1998). "Plastic-Damage Model for Cyclic Loading of Concrete Structures", *Journal of Engineering Mechanics, ASCE*, Vol. 124, No. 8, pp. 892–900.
15. Lubliner, J., Oliver, J., Oller, S. and Onate, E. (1989). "A Plastic-Damage Model for Concrete", *International Journal of Solids and Structures*, Vol. 25, No. 3, pp. 229–326.
16. Skrikerud, P.E. and Bachmann, H. (1986). "Discrete Crack Modeling for Dynamically Loaded, Unreinforced Concrete Structures", *Earthquake Engineering & Structural Dynamics*, Vol. 14, No. 2, pp. 297–315.
17. Zienkiewicz, O.C., Emson, C. and Bettess, P. (1983). "A Novel Boundary Infinite Element", *International Journal for Numerical Methods in Engineering*, Vol. 19, No. 3, pp. 393–404.